Editors' Suggestion

Geometric Bound on the Efficiency of Irreversible Thermodynamic Cycles

Adam G. Frim[1,*] and Michael R. DeWeese[1,2,3,†]
[1]Department of Physics, University of California, Berkeley, Berkeley, California, 94720
[2]Redwood Center For Theoretical Neuroscience, University of California, Berkeley, Berkeley, California, 94720
[3]Helen Wills Neuroscience Institute, University of California, Berkeley, Berkeley, California, 94720

(Received 3 January 2022; accepted 17 May 2022; published 8 June 2022)

Stochastic thermodynamics has revolutionized our understanding of heat engines operating in finite time. Recently, numerous studies have considered the optimal operation of thermodynamic cycles acting as heat engines with a given profile in thermodynamic space (e.g., $P-V$ space in classical thermodynamics), with a particular focus on the Carnot engine. In this work, we use the lens of thermodynamic geometry to explore the full space of thermodynamic cycles with continuously varying bath temperature in search of optimally shaped cycles acting in the slow-driving regime. We apply classical isoperimetric inequalities to derive a universal geometric bound on the efficiency of any irreversible thermodynamic cycle and explicitly construct efficient heat engines operating in finite time that nearly saturate this bound for a specific model system. Given the bound, these optimal cycles perform more efficiently than all other thermodynamic cycles operating as heat engines in finite time, including notable cycles, such as those of Carnot, Stirling, and Otto. For example, in comparison to recent experiments, this corresponds to orders of magnitude improvement in the efficiency of engines operating in certain time regimes. Our results suggest novel design principles for future mesoscopic heat engines and are ripe for experimental investigation.

DOI: 10.1103/PhysRevLett.128.230601

Introduction.—Over the past several decades, stochastic thermodynamics has dramatically improved our understanding of nonequilibrium statistical physics [1–7]. A major focus of study in this area has been the performance of engines operating in finite time, where both power and dissipation are finite, often with an emphasis on engines operating at maximal power [8–24]. A recurring theme has been the interplay, and often incompatibility, among high efficiency, high output power, and low dissipation [13,15,18,22]. To that end, we recently characterized optimal protocols for the finite-time operation of a Brownian Carnot engine [22], a colloidal system introduced in Ref. [25], finding minimally dissipative cycles often came at the expense of reduced power and efficiency.

In this work, we study the implications of this interplay from a geometric perspective and arrive at a universal bound on the efficiency of heat engines operating in finite time. We also numerically construct optimal cycles that nearly saturate the bound, and we characterize its tightness for a specific model system and compare them to a variety of nonoptimal cycles. We find that even natural extensions of well-known quasistatic cycles (e.g., Carnot engines) to finite-time cycles perform far less efficiently than the optimal cycles, demonstrating the utility of our result.

Efficiency of irreversible engines.—Following Ref. [26], we use a definition of efficiency that directly captures the irreversibility of a thermodynamic cycle. Specifically, for a generic thermodynamic engine operated by cyclically varying the temperature T of a heat bath in contact with the system and some volumelike mechanical control variable λ, the (average) efficiency is defined as

$$\eta \equiv \frac{W}{U} = \frac{\oint X_\lambda d\lambda}{\oint X_T dT}, \tag{1}$$

where X_ν is the thermodynamic force conjugate to the control variable $\nu \in \{T, \lambda\}$, defined as

$$X_\lambda \equiv -\left\langle \frac{\partial H_{\mathbf{\Lambda}}}{\partial \lambda} \right\rangle, \tag{2}$$

$$X_T = S \equiv -\langle \log \rho_t \rangle, \tag{3}$$

where $H_{\mathbf{\Lambda}}$ is the Hamiltonian of the (working) system for a fixed set $\mathbf{\Lambda} = (T, \lambda)$, S is the system entropy, ρ_t is the phase space distribution of the system at time t, and brackets denote ensemble averages. Note that U here does not represent the internal energy, but can be thought of as the uptake of thermal energy from the heat source, or the amount of energy that is available for work production under a given temperature profile [26]. This efficiency is well defined for any engine with positive work output, $W > 0$. Following the first law of thermodynamics and appealing to the cyclic operation of the engine, the efficiency may be rewritten as

$$\eta = \frac{\oint X_\lambda d\lambda}{\oint S dT} = \frac{\oint X_\lambda d\lambda}{\oint X_\lambda d\lambda + \oint T d\Sigma} \leq 1, \tag{4}$$

where $d\Sigma \equiv dS - dQ/T$ is the total infinitesimal entropy production in the universe. Here, Q is the heat exchange into the system from the reservoir at a temperature T. Following the second law, $d\Sigma \geq 0$ such that the inequality follows directly and the unity bound can only be saturated for quasistatic, reversible engines. This definition of efficiency has gained traction in the study of finite-time heat engines [21,22,27], and a comparable definition is standard for monothermal cycles, e.g., in active matter or chemical transduction contexts [28–31].

Now, let us consider a finite-time operation such that $\Sigma > 0$ and the system is driven with finite driving rates $\dot{\mathbf{\Lambda}}$. The thermodynamic forces may be expanded as

$$X_\mu = \mathcal{X}_\mu - g_{\mu\nu}\dot{\Lambda}_\nu, \tag{5}$$

where summation over repeated indices is implied. Here, $\mathcal{X}_\mu$ is the quasistatic value of X for a given set $\mathbf{\Lambda}$ and, following the standard linear response framework, $g_{\mu\nu}$ is given by a correlation function

$$g_{\mu\nu} = \beta \int_0^\infty dt \langle \delta X_\mu(t) \delta X_\nu(0) \rangle_{\mathbf{\Lambda}}. \tag{6}$$

Using this expansion, the efficiency can be written

$$\eta = \frac{\oint X_\lambda d\lambda}{\oint X_T dT} \approx \frac{\oint (\mathcal{X}_\lambda - g_{\lambda\nu}\dot{\Lambda}_\nu) d\lambda}{\oint (\mathcal{X}_T - g_{T\nu}\dot{\Lambda}_\nu) dT} \approx 1 - \frac{\oint dt \dot{\Lambda}_\mu g_{\mu\nu} \dot{\Lambda}_\nu}{\oint \mathcal{X}_\lambda d\lambda}$$
$$= 1 - \frac{A}{\mathcal{W}}, \tag{7}$$

where A is the dissipated work (or alternatively called the dissipated availability) through one cycle and $\mathcal{W}$ is the work output for quasistatic driving. Following Refs. [32–39], we see that the thermodynamic control space is imbued with a geometric structure by reinterpreting $g_{\mu\nu}$ as a metric tensor. Geometric approaches such as this have greatly facilitated the development of optimal protocols for nonequilibrium systems [38–47]. With these definitions, the dissipated work satisfies

$$\tau A \equiv \tau \oint dt \dot{\Lambda}_\mu g_{\mu\nu} \dot{\Lambda}_\nu \geq \left(\oint dt \sqrt{\dot{\Lambda}_\mu g_{\mu\nu} \dot{\Lambda}_\nu} \right)^2 \equiv \mathcal{L}^2, \tag{8}$$

where τ is the cycle duration and $\mathcal{L}$ is the *thermodynamic length* of the protocol as defined by the metric. Optimal driving then yields [26]

$$\eta \leq \eta^* = 1 - \frac{\mathcal{L}^2}{\mathcal{W}\tau}, \tag{9}$$

which gives the optimal geometric efficiency η^* for any closed curve in thermodynamic control space.

The bound, Eq. (9), applies to any generic closed curve, yielding the best possible efficiency for an optimal temporal parametrization for a given path. We now seek to go further and find cycles that are maximally efficient over the space of all possible closed paths in thermodynamic control space. Fixing the protocol duration and given Eq. (9), to leading order in $1/\tau$, we must therefore find the curve that minimizes the quantity $\mathcal{L}^2/\mathcal{W}$.

Isoperimetric bound on efficiency.—We now note an important feature of $\mathcal{W}$. It is well known from standard thermodynamics that the quasistatic work is simply given by the area contained within the curve of the (quasistatic) cycle in $\lambda - \mathcal{X}_\lambda$ space, which we will henceforth refer to as Clausius space in reference to the Clausius curve. We will refer to the inner region of this curve as $\mathcal{C}$ and the boundary (the Clausius curve) as $\partial\mathcal{C}$. By means of an appropriate change of coordinates, the metric $g_{\mu\nu}$ may be transformed for this space, yielding a metric $g^{\mathcal{C}}_{\mu\nu}$ such that the thermodynamic length is given

$$\mathcal{L} = \oint_{\partial\mathcal{C}} \sqrt{\begin{pmatrix} dT \\ d\lambda \end{pmatrix}_\mu g_{\mu\nu} \begin{pmatrix} dT \\ d\lambda \end{pmatrix}_\nu}$$
$$= \oint_{\partial\mathcal{C}} \sqrt{\begin{pmatrix} d\mathcal{X}_\lambda \\ d\lambda \end{pmatrix}_\mu g^{\mathcal{C}}_{\mu\nu} \begin{pmatrix} d\mathcal{X}_\lambda \\ d\lambda \end{pmatrix}_\nu}, \tag{10}$$

and the quasistatic work is

$$\mathcal{W} = \iint_{\mathcal{C}} d\lambda d\mathcal{X}_\lambda = \oint_{\partial\mathcal{C}} \mathcal{X}_\lambda d\lambda. \tag{11}$$

We define one final quantity of interest: the thermodynamic area, defined as the integral over of the region with the proper thermodynamic geometric measure:

$$\mathcal{A} = \iint_{\mathcal{C}} \sqrt{g^{\mathcal{C}}} d\lambda d\mathcal{X}_\lambda, \tag{12}$$

where $g^{\mathcal{C}} \equiv \det g^{\mathcal{C}}_{\mu\nu}$. The physical interpretation of this quantity may not be as clear as that of thermodynamic length, though we will use it as a key ingredient. Notably, dating to antiquity [48,49], bounds exist relating the perimeter $\mathcal{L}(D)$ and area $\mathcal{A}(D)$ of a region D, known as *isoperimetric inequalities*. In general, for a simply-connected two-dimensional region, one has two inequalities [49]

$$\mathcal{L}^2 \geq 4\pi\mathcal{A} - 2\left[\iint_D K^+\right]\mathcal{A}, \tag{13}$$

$$\mathcal{L}^2 \geq 4\pi\mathcal{A} - [\sup_D K]\mathcal{A}^2. \tag{14}$$

where K is the Gaussian curvature of the underlying space and $K^+(p) \equiv \max[K(p), 0]$ for a point $p \in D$. As a simple example, we remind the reader of the case of Euclidean space where $K = K^+ = 0$ and both inequalities yield $\mathcal{L}^2 \geq 4\pi\mathcal{A}$, which is saturated only for the optimal shape of a circle. Similar isoperimetrically optimal shapes exist for other manifolds [49]. Importantly, whenever the curvature is everywhere nonpositive, Eq. (13) yields the familiar Euclidean bound, though it is only tight for special spaces, such as when $K = 0$.

In the context of thermodynamic geometry, the bound readily applies, where now we consider the thermodynamic length of a closed curve and the thermodynamic area of the enclosed region. That is,

$$\mathcal{L}^2 \geq 4\pi\mathcal{A} - 2\left[\iint_{\mathcal{C}} K^+\right]\mathcal{A}, \tag{15}$$

$$\mathcal{L}^2 \geq 4\pi\mathcal{A} - [\sup_{\mathcal{C}} K]\mathcal{A}^2. \tag{16}$$

Henceforth, we will focus on the case when $K \leq 0$ and will relegate the more general case to the Supplemental Material [50]. In this case, we may assume $\mathcal{L}^2 \geq 4\pi\mathcal{A}$. Therefore,

$$\frac{\mathcal{L}^2}{\mathcal{W}} = \frac{\mathcal{L}^2}{\mathcal{W}}\frac{\mathcal{A}}{\mathcal{A}} = \frac{\mathcal{L}^2}{\mathcal{A}}\frac{\mathcal{A}}{\mathcal{W}} \geq 4\pi\frac{\mathcal{A}}{\mathcal{W}} = 4\pi\sqrt{\bar{g^{\mathcal{C}}}}, \tag{17}$$

where the overline indicates an area average value. Given this bound, we may now write for the efficiency a universal bound

$$\eta \leq 1 - \frac{\mathcal{L}^2}{\mathcal{W}\tau} \leq 1 - \frac{4\pi\sqrt{\bar{g^{\mathcal{C}}}}}{\tau}. \tag{18}$$

This bound, which we will refer to as an isoperimetric bound on efficiency, is our first major result and presents a fundamentally new and purely geometric bound on the efficiency of nonequilibrium engines. Also, whereas the previous bound, Eq. (9), was directly applicable to the optimized parametrization of a specific predetermined cycle, this bound places constraints on the optimal *shape* of a cycle and can only be approached for geometrically optimized cycle shapes. This therefore introduces a new optimization principle wherein optimally efficient cycles must minimize the average value of $\sqrt{g^{\mathcal{C}}}$ over the region they enclose in Clausius space. In a pioneering study, a similar bound was recently recovered for the specific case of the Brownian gyrator [27], though we highlight that Eq. (18) applies generically.

Construction of optimal cycles.—Given this isoperimetric bound, we now seek to construct optimal cycles that (nearly) saturate it. This is done by finding shapes that minimize the ratio $\mathcal{L}^2/\mathcal{A}$. Inspired by previous literature [49], we will use a variational principle. Namely, we seek to maximize $\mathcal{A}$ while holding $\mathcal{L}^2$ fixed; we do so by means of a Lagrange multiplier. The relevant functional takes the form

$$\mathcal{F} = \oint dt\left[\sqrt{g^{\mathcal{C}}}X_\lambda\dot{\lambda} - \xi\begin{pmatrix}\dot{X}_\lambda \\ \dot{\lambda}\end{pmatrix}_\mu g^{\mathcal{C}}_{\mu\nu}\begin{pmatrix}\dot{X}_\lambda \\ \dot{\lambda}\end{pmatrix}_\nu\right], \tag{19}$$

where ξ serves as a Lagrange multiplier enforcing a fixed dissipation for shapes that maximize the corresponding area [51]. Optimization is found through solving the resulting Euler-Lagrange equations for $X_\lambda(t)$ and $\lambda(t)$ under a cyclic constraint.

Parametric harmonic oscillator.—We will now illustrate the utility of this result by studying the parametric harmonic oscillator. This important model system consists of a particle of mass m trapped in a harmonic potential with variable stiffness $V(x) = 1/2k(t)x^2$ in contact with a heat bath of variable temperature $T(t)$ and subject to viscous damping ζ. This system has been studied extensively [22,25,40,52–56], and its geometry has been well characterized—the metric is

$$g_{\mu\nu} = \frac{mk_B}{4\zeta}\begin{pmatrix}\frac{1}{T}\left(4 + \frac{(\zeta)^2}{km}\right) & -\frac{1}{k}\left(2 + \frac{(\zeta)^2}{km}\right) \\ -\frac{1}{k}\left(2 + \frac{(\zeta)^2}{km}\right) & \frac{T}{k^2}\left(1 + \frac{(\zeta)^2}{km}\right)\end{pmatrix}_{\mu\nu}.$$

In this case, the mechanical control variable is k and the corresponding force is $X_k = -1/2\langle x^2\rangle$. In the quasistatic limit, we have $\mathcal{X}_k = -k_BT/2k$ by the equipartition theorem. Therefore, under the change of variables $(T, k) \to (\tilde{P}, \tilde{V}) \equiv (\mathcal{X}_k, k)$, we find

$$g^{\mathcal{C}}_{\mu\nu} = -\begin{pmatrix}\frac{\zeta}{2\tilde{P}} + \frac{2m\tilde{V}}{\zeta\tilde{P}} & \frac{m}{\zeta} \\ \frac{m}{\zeta} & \frac{m\tilde{P}}{2\zeta\tilde{V}}\end{pmatrix},$$

where we use $\tilde{P}$ and $\tilde{V}$ to suggestively map to pseudopressure and pseudovolume in Clausius space and recapture the usual identity $d\mathcal{W} = \tilde{P}d\tilde{V}$. We find $g^{\mathcal{C}} = m/(4\tilde{V})$ and the Gaussian curvature $K = 1/(\zeta\tilde{P}) \leq 0$ as $\tilde{P} \leq 0$ such that Eq. (18) applies. As a result, we have

$$\eta \leq 1 - \frac{2\pi\sqrt{\bar{\frac{m}{\tilde{V}}}}}{\tau}$$

for any possible thermodynamic cycle.

We now seek to characterize the optimal cycles for this model system. Following Eq. (19), we consider the functional

$$\mathcal{F} = \oint dt\left[\sqrt{g^{\mathcal{C}}}\tilde{P}\dot{\tilde{V}} + \xi\begin{pmatrix}\dot{\tilde{P}} \\ \dot{\tilde{V}}\end{pmatrix}\begin{pmatrix}\frac{\zeta}{2\tilde{P}} + \frac{2m\tilde{V}}{\zeta\tilde{P}} & \frac{m}{\zeta} \\ \frac{m}{\zeta} & \frac{m\tilde{P}}{2\zeta\tilde{V}}\end{pmatrix}\begin{pmatrix}\dot{\tilde{P}} \\ \dot{\tilde{V}}\end{pmatrix}\right]. \tag{20}$$

The Euler-Lagrange equations are then found by varying with respect to $\tilde{P}$ and $\tilde{V}$ (Supplemental Material [50]). To our knowledge, the resulting Euler-Lagrange equations are analytically intractable, so we turn to numerics. For simplicity, we generate cycles from a given set of initial conditions, $\tilde{P}(0)$, $\tilde{V}(0)$, $\dot{\tilde{P}}(0)$, and $\dot{\tilde{V}}(0)$, and a given value of the Lagrange multiplier ξ. If we concern ourselves only with the shape of the curve rather than its particular parametrization, we could instead parametrize $\tilde{P}$ as a function of $\tilde{V}$, such that one of these initial condition degrees of freedom is redundant. Thus, optimal shapes are specified by a four-parameter family determined by $\tilde{P}(t=0)$, $\tilde{V}(t=0)$, $d\tilde{P}/d\tilde{V}(t=0)$, and ξ.

Generically, it is unclear whether these conditions will be sufficient to specify a smooth closed curve [48,49,57]. In general, the isoperimetrically optimal curves will consist of stable smooth curves that have constant geodesic curvature at (nearly) all points [48,49,57]. In our case, the numerical solutions yield curves of constant geodesic curvature that are typically nonclosed but instead consist of "near-miss" cycloids [50], which has been observed previously while seeking optimal cycles [56]. However, as we are interested only in cyclic engines, we will construct cycles that traverse a single optimal period by truncating the curve when it is at the nearest point on the curve whose tangent curve is parallel to the original tangent curve. We then connect these two points by a straight line, thus closing the cycle. For small cycles, the resulting kink is imperceptible whereas it becomes more noticeable for larger cycles, as can be seen in Figs. 1 and 2. Similarly, the efficiencies are impacted more significantly for larger deviations from smooth curves. Truly optimal curves would consist of fully smooth closed curves of constant geodesic curvature, which may only be realizable in specific regions of the Clausius space. By choosing to work with specific initial conditions, we allow for the construction of near optimal cycles at all points of Clausius space at the cost of having to introduce small, finite sections of nonoptimality. As we will see, these "optimal" cycles still prove remarkably close to saturating the bound and strongly outperform all other cycles we consider.

For example, consider the Brownian Carnot cycle, whose shape is given in Fig. 1. Setting $\zeta = 7.51\ \mu\mathrm{g\,s^{-1}}$ and $m = 0.545$ pg (based on experimental parameters used in Ref. [25]), and choosing the extremal values of $\tilde{P}$ and $\tilde{V}$ shown, Eq. (17) implies that its greatest possible efficiency is

$$(1-\eta)\tau = \frac{\mathcal{L}^2}{\mathcal{W}} = 9.58\times10^{-4}\ \mathrm{s} \gg 1.76\times10^{-5}\ \mathrm{s} = \frac{4\pi\mathcal{A}}{\mathcal{W}},$$

demonstrating that the performance of the Carnot cycle is a factor of 55 times larger than the optimal value for these parameter settings. In contrast, by constructing a series of (nearly) optimally shaped cycles with identical values of $\mathcal{W}$ and $\overline{\sqrt{g^{\mathcal{C}}}}$, we instead find the bound is approached to within three-hundredths of one percent. The shapes of these cycles are displayed in Fig. 1(a).

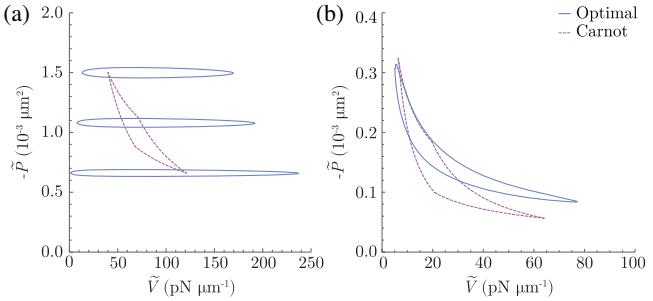

FIG. 1. (a) A Brownian Carnot cycle (dashed purple) and three isoperimetrically optimal cycles (blue) with identical values of $\mathcal{W}$ and $\overline{\sqrt{g^{\mathcal{C}}}}$ using mass and damping values from Ref. [25]. The optimal cycles have a 55× increase in performance relative to the Carnot cycle. (b) Same as (a), but in a more underdamped regime.

We next consider a slightly underdamped parameter regime, setting $m = 80.9$ mg and $\zeta = 15.0\ \mathrm{mg\,s^{-1}}$. In this regime, various Carnot engine cycles (for given limits on hot and cold bath temperature) perform somewhat better, but they still do not come close to saturating it. Intriguingly, in contrast to the previous regime, optimally constructed shapes now appear much closer to Carnot-like cycles than those previously constructed, as in Fig 1(b). Now, we find that optimal engines seemingly remain close to adiabats for a significant duration of the cycle, albeit with a rapid (and smooth) turnaround at corners. This is replicated for other choices of maximal temperature and stiffness as shown in Fig. 1(b). We also show optimal cycles for a variety of values of m/ζ in the Supplemental Material [50].

We can further evaluate our bound by comparing it to generic cycles in Clausius space. In particular, in Fig. 3, we plot the value of $\overline{\sqrt{g^{\mathcal{C}}}}$ against $\mathcal{L}^2/\mathcal{W}$ for 15 000 randomly constructed cycles, as well as 1000 randomly selected Carnot, Stirling, Otto, and hybrid Carnot-geodesic (introduced in Ref. [22]) cycles (see Ref. [50] for a review of

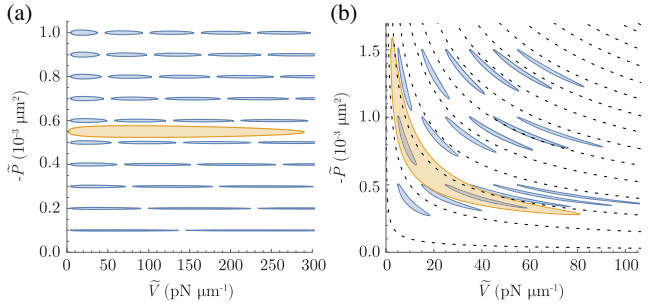

FIG. 2. (a) Optimally constructed cycles with quasistatic output work of 6 (blue) and 120 pNμm (orange) for experimental parameters used in Ref. [25]. (b) Same as (a) for underdamped parameters; adiabats shown in dotted lines.

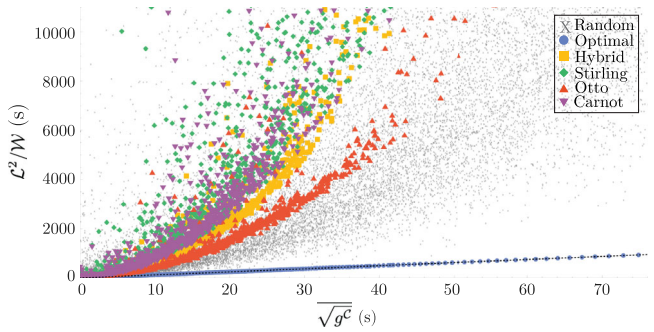

FIG. 3. Optimally constructed cycles strongly outperform Carnot and all other cycles tested. Optimal (blue circles), hybrid (orange squares), Stirling (green diamonds), Otto (red upwards triangle), Carnot (purple downwards triangle), and randomly constructed (gray X's) plotted against the bound Eq. (17) (black dotted line).

these various cycles and for details of how Fig. 3 is constructed). We also plot 500 optimally constructed cycles. As is easily observed, the optimal cycles nearly saturate the bound for a large parameter regime of $\overline{\sqrt{g^{\mathcal{C}}}}$ whereas other cycles are far less efficient. The data are surprisingly structured: for a fixed shape, we find $\mathcal{L}^2/\mathcal{W} \sim (\overline{\sqrt{g^{\mathcal{C}}}})^2$, an interesting empirical finding. Cycles that saturate the bound must therefore *not* maintain the same cyclical shape for different average values of $\sqrt{g^{\mathcal{C}}}$, but instead change so as to remain optimal, as was shown in Fig. 2.

Discussion.—In this work, we have applied the classical isoperimetric inequalities to thermodynamic spaces, yielding a novel universal bound on the efficiency of any closed thermodynamic cycle for a generic system. We have then constructed optimal cycles that nearly saturate this bound for the specific model system of the parametric harmonic oscillator. Importantly, this bound, although not always tight, nevertheless strongly constrains the efficiency of thermodynamic cycles and introduces new design principles for the design of efficient finite-time heat engines. We emphasize that all results are independent of temporal parametrization and depend only on the shape of cycles.

This derivation ultimately arises from thermodynamic geometry, which is a perturbative solution to first order in response theory. Our bound is therefore only approximate in nature and does not technically constrain the efficiency of engines acting beyond slow driving. However, it is unlikely such engines would prove less dissipative and more efficient than their slower-driven counterparts, such that one would expect the bound to still apply, but not be as tight. A more interesting question is whether there are higher order or even nonperturbative bounds that constrain the efficiency of all finite time cycles. Such bounds have been found for the fluctuations of the more traditional definition of efficiency about its mean [58–60]. Similarly, one should ask if the efficiency of optimal engines in our framework would still outperform others, such as the Carnot or Stirling engine, even when far away from linear response where our results are not guaranteed to apply. We leave the detailed study of the question to future work, but there does exist anecdotal evidence that engines designed in linear response prove more efficient, even when operating far from equilibrium [22,26].

Also, although the main focus of this work was in optimizing the average efficiency of thermodynamic cycles, given that our optimal cycles were designed to be minimally dissipative for a fixed thermodynamic area, they should also have a high output power, though they may not be *optimally* powerful cycles. A recurring theme in the literature is the set of tradeoffs between high output power, high efficiency, low dissipation, and minimal fluctuations about the means of stochastic thermodynamic quantities [17,20,23,24,26,46,60,61]. Studying this interplay further and designing optimal cycles achieving different objectives is of interest for future work. Similarly, we focused on the problem of finding optimal, unconstrained cycles in thermodynamic space, such that control parameters, the temperature of the heat bath and mechanical controls, are allowed to vary continuously in time. Although this regime has been studied extensively [13,21–23,26] and is experimentally accessible [25], it is a distinct and worthwhile question to address the problem of constructing optimal, finite-time engines under other more constrained control settings where such smooth variations may not be possible.

In addition and more generally, isoperimetric inequalities have been a significant direction of study in mathematics, and we expect them to have important implications in thermodynamic geometry. We are encouraged by their recent application to the Brownian gyrator [27] and adiabatic thermal engines operating between two heat baths [24], but we anticipate there remains a great deal to be learned by their application in various thermodynamic settings. In particular, whereas ultimately our bound relied on the introduction of thermodynamic area, isoperimetric inequalities for manifolds with density [50,62–64] could lead to further strict bounds on dissipation directly given a work output.

Finally, although our main focus here was on classical thermal systems, thermodynamic geometry is equally applicable to quantum settings and this bound likewise should constrain the efficiency of quantum heat engines, a major focus of current research [18,46,65–68].

Conclusion.—Here, we have used classical geometric results in concert with geometric approaches to thermodynamics to place a bound on the efficiency of any irreversible heat engine and study it in the specific case of the parametric harmonic oscillator. This bound applies irrespective of the system details or dynamics and it suggests new design principles for construction of efficient engines at microscopic scales.

The authors thank Jamie Simon, Adrianne Zhong, Martí Perarnau-Llobet, and Aaron Slipper for many useful discussions and thank Gentaro Watanabe and Yuki Minami for comments on the manuscript. The authors also acknowledge the attendees of the 2021 Telluride Information Engines Workshop for useful comments at preliminary stages of this work. A. G. F. is supported by the NSF GRFP under Grant No. DGE 1752814. This work was supported in part by the U.S. Army Research Laboratory and the U.S. Army Research Office under Contract No. W911NF-20-1-0151.

*adamfrim@berkeley.edu
†deweese@berkeley.edu

[1] C. Jarzynski, Phys. Rev. Lett. **78**, 2690 (1997).
[2] K. Sekimoto, Prog. Theor. Phys. Suppl. **130**, 17 (1998).
[3] G. E. Crooks, Phys. Rev. E **60**, 2721 (1999).
[4] U. Seifert, Phys. Rev. Lett. **95**, 040602 (2005).
[5] M. Esposito and C. Van den Broeck, Phys. Rev. Lett. **104**, 090601 (2010).
[6] T. Sagawa and M. Ueda, Phys. Rev. Lett. **104**, 090602 (2010).
[7] U. Seifert, Rep. Prog. Phys. **75**, 126001 (2012).
[8] F. L. Curzon and B. Ahlborn, Am. J. Phys. **43**, 22 (1975).
[9] C. Van den Broeck, Phys. Rev. Lett. **95**, 190602 (2005).
[10] T. Schmiedl and U. Seifert, Europhys. Lett. **81**, 20003 (2008).
[11] M. Esposito, K. Lindenberg, and C. Van den Broeck, Phys. Rev. Lett. **102**, 130602 (2009).
[12] M. Esposito, R. Kawai, K. Lindenberg, and C. Van den Broeck, Phys. Rev. Lett. **105**, 150603 (2010).
[13] K. Brandner, K. Saito, and U. Seifert, Phys. Rev. X **5**, 031019 (2015).
[14] K. Proesmans, B. Cleuren, and C. Van den Broeck, Phys. Rev. Lett. **116**, 220601 (2016).
[15] N. Shiraishi, K. Saito, and H. Tasaki, Phys. Rev. Lett. **117**, 190601 (2016).
[16] Y.-H. Ma, D. Xu, H. Dong, and C.-P. Sun, Phys. Rev. E **98**, 022133 (2018).
[17] Y.-H. Ma, D. Xu, H. Dong, and C.-P. Sun, Phys. Rev. E **98**, 042112 (2018).
[18] P. Abiuso and M. Perarnau-Llobet, Phys. Rev. Lett. **124**, 110606 (2020).
[19] Y.-H. Ma, R.-X. Zhai, J. Chen, C. P. Sun, and H. Dong, Phys. Rev. Lett. **125**, 210601 (2020).
[20] H. J. D. Miller and M. Mehboudi, Phys. Rev. Lett. **125**, 260602 (2020).
[21] O. Movilla Miangolarra, R. Fu, A. Taghvaei, Y. Chen, and T. T. Georgiou, Phys. Rev. E **103**, 062103 (2021).
[22] A. G. Frim and M. R. DeWeese, Phys. Rev. E **105**, L052103 (2022).
[23] G. Watanabe and Y. Minami, Phys. Rev. Research **4**, L012008 (2022).
[24] P. Terrén Alonso, P. Abiuso, M. Perarnau-Llobet, and L. Arrachea, PRX Quantum **3**, 010326 (2022).
[25] I. A. Martínez, É. Roldán, L. Dinis, D. Petrov, J. M. R. Parrondo, and R. A. Rica, Nat. Phys. **12**, 67 (2016).
[26] K. Brandner and K. Saito, Phys. Rev. Lett. **124**, 040602 (2020).
[27] O. Movilla Miangolarra, A. Taghvaei, R. Fu, Y. Chen, and T. T. Georgiou, Phys. Rev. E **104**, 044101 (2021).
[28] P. Pietzonka, A. C. Barato, and U. Seifert, J. Stat. Mech. (2016) 124004.
[29] P. Pietzonka, E. Fodor, C. Lohrmann, M. E. Cates, and U. Seifert, Phys. Rev. X **9**, 041032 (2019).
[30] T. Ekeh, M. E. Cates, and E. Fodor, Phys. Rev. E **102**, 010101(R) (2020).
[31] J. S. Lee, J.-M. Park, and H. Park, Phys. Rev. E **102**, 032116 (2020).
[32] F. Weinhold, J. Chem. Phys. **63**, 2479 (1975).
[33] G. Ruppeiner, Phys. Rev. A **20**, 1608 (1979).
[34] P. Salamon and R. S. Berry, Phys. Rev. Lett. **51**, 1127 (1983).
[35] P. Salamon, J. Nulton, and E. Ihrig, J. Chem. Phys. **80**, 436 (1984).
[36] F. Schlögl, Z. Phys. B Condens. Matter **59**, 449 (1985).
[37] G. Ruppeiner, Rev. Mod. Phys. **67**, 605 (1995).
[38] G. E. Crooks, Phys. Rev. Lett. **99**, 100602 (2007).
[39] D. A. Sivak and G. E. Crooks, Phys. Rev. Lett. **108**, 190602 (2012).
[40] P. R. Zulkowski, D. A. Sivak, G. E. Crooks, and M. R. DeWeese, Phys. Rev. E **86**, 041148 (2012).
[41] P. R. Zulkowski and M. R. DeWeese, Phys. Rev. E **89**, 052140 (2014).
[42] P. R. Zulkowski, D. A. Sivak, and M. R. DeWeese, PLoS One **8**, e82754 (2013).
[43] P. R. Zulkowski and M. R. DeWeese, Phys. Rev. E **92**, 032113 (2015).
[44] P. R. Zulkowski and M. R. DeWeese, Phys. Rev. E **92**, 032117 (2015).
[45] G. M. Rotskoff and G. E. Crooks, Phys. Rev. E **92**, 060102 (R) (2015).
[46] P. Abiuso, H. J. D. Miller, M. Perarnau-Llobet, and M. Scandi, Entropy **22**, 1076 (2020).
[47] S. Blaber and D. A. Sivak, J. Chem. Phys. **153**, 244119 (2020).
[48] L. E. Payne, SIAM Rev. **9**, 453 (1967).
[49] R. Osserman, Bull. Am. Math. Soc. **84**, 1182 (1978).
[50] See Supplemental Material at http://link.aps.org/supplemental/10.1103/PhysRevLett.128.230601 for further details on derivations, numerical methods, isoperimetric bounds for arbitrary curvatures, and the potential future thermodynamic uses for manifolds with density.
[51] The dissipation $\oint (dX_\lambda, d\lambda) \cdot \mathbf{g} \cdot (dX_\lambda, d\lambda)$ is geometrically denoted the energy of the curve and optimization with respect to its value held fixed still optimizes the ratio $\mathcal{L}^2/\mathcal{A}$ while simultaneously outputting an optimal, arclength parametrization of the resultant curve.
[52] T. Schmiedl and U. Seifert, Phys. Rev. Lett. **98**, 108301 (2007).
[53] V. Blickle and C. Bechinger, Nat. Phys. **8**, 143 (2012).
[54] I. A. Martínez, E. Roldán, L. Dinis, D. Petrov, and R. A. Rica, Phys. Rev. Lett. **114**, 120601 (2015).
[55] I. A. Martínez, E. Roldán, L. Dinis, and R. A. Rica, Soft Matter **13**, 22 (2017).
[56] Y. Huang and P. S. Krishnaprasad, Discrete Contin. Dyn. Syst.—S **13**, 1243 (2020).
[57] M. Ritoré, Commun. Anal. Geom. **9**, 1093 (2001).

[58] G. Verley, T. Willaert, C. Van den Broeck, and M. Esposito, Phys. Rev. E **90**, 052145 (2014).
[59] K. Ito, C. Jiang, and G. Watanabe, arXiv:1910.08096.
[60] S. Saryal, M. Gerry, I. Khait, D. Segal, and B. K. Agarwalla, Phys. Rev. Lett. **127**, 190603 (2021).
[61] P. Pietzonka and U. Seifert, Phys. Rev. Lett. **120**, 190602 (2018).
[62] F. Morgan, Not. Am. Math. Soc. **52**, 853 (2005), https://www.ams.org/journals/notices/200508/fea-morgan.pdf.
[63] C. Rosales, A. Cañete, V. Bayle, and F. Morgan, Calc. Var. Partial Differ. Equ. **31**, 27 (2008).
[64] F. Morgan and A. Pratelli, Ann. Glob. Anal. Geom. **43**, 331 (2013).
[65] R. Kosloff and A. Levy, Annu. Rev. Phys. Chem. **65**, 365 (2014).
[66] B. Gardas and S. Deffner, Phys. Rev. E **92**, 042126 (2015).
[67] S. Deffner, Entropy **20**, 875 (2018).
[68] H. J. D. Miller, M. H. Mohammady, M. Perarnau-Llobet, and G. Guarnieri, Phys. Rev. Lett. **126**, 210603 (2021).